ALT 12
Advanced Laser Technologies
2 – 6 September 2012, Thun, Switzerland

ALT 12
c/o Bern University of Applied Sciences
Engineering and Information Technology
Pestalozzistrasse 20, CH-3400 Burgdorf
info@alt12.org, www.alt12.org
0041 (0) 34 426 42 06

PHOTOACOUSTIC SECTION IMAGING WITH INTEGRATING DETECTORS

Authors:

G. Paltauf, R. Nuster, S. Gratt

DOI: 10.12684/alt.1.93

Corresponding author: G. Paltauf

e-mail: guenther.paltauf@uni-graz.at

Photoacoustic section imaging with integrating detectors

G. Paltauf, R. Nuster, S. Gratt

Department of Physics, Karl-Franzens-Universitaet Graz,
Universitaetsplatz 5, Graz, 8010, Austria
[2]Institution, Address, City, State, Postal Code, Country

Abstract

Photoacoustic section imaging is a method for visualizing structures with optical contrast in selected layers of an extended object. In order to avoid resolution limitations that are due to commonly used ultrasound detectors of finite size, we propose the use of extended, integrating cylindrical elements for focusing the acoustic detection into the selected section. Two imaging methods based on piezoelectric and optical detection are presented. Resolution limits and results on zebra fish are demonstrated.

Introduction

Photoacoustic or optoacoustic imaging is a method to visualize absorbing structures in optically turbid objects [1]. It is based on the generation of acoustic waves by absorption of electromagnetic radiation. Usually, pulsed laser sources are used to irradiate the object and the emitted sound waves are measured with broadband acoustic detectors around the object to be imaged. A reconstruction algorithm is used to localize the absorbing structures. The method is very promising for the imaging of biological tissue. For three-dimensional (3D) tomography, the amount of data needed for a reconstruction is very large, because measurements have to be taken on a closed surface surrounding the object.

An alternative is two-dimensional (2D) section imaging, where the detection of acoustic waves is limited to a section or a thin slab within the investigated object [2,3]. This is achieved by use of cylindrical lens detectors, which are rotated or arranged on a circle surrounding the object. Reconstruction of the deposited electromagnetic energy within the section is done by back projecting the recorded signals onto circles around the detector positions with radius $c_s \cdot t$, where c_s is the speed of sound and t the time after the laser pulse, which is also the time of flight of the acoustic wave from a source to the detector. Such a back projection is, however, only exact if the sensor has negligible size and can be assumed to be a point. If this is not the case, the image becomes blurred at the periphery, at points lying at some distance from the center of the detection circle [4].

A way to avoid this blurring is the use of extended detectors. These integrating detectors are larger than the object [5]. For section imaging, a typical implementation of such a detector is shown in Fig. 2. It is a lens less, cylindrically focusing piezoelectric element, with an extension in direction of the cylinder axis exceeding the size of the object to be imaged. In this way a registered signal at a given time is related to an integral of the initial pressure distribution along direction of the cylinder axis [6]. For reconstruction from a set of measurements at different orientations of the sensor relative to the object, the inverse Radon transform is used. Photoacoustic section imaging with such a detector is therefore related to various tomographic methods that are based on straight projections, such as X-ray tomography or positron emission tomography (PET).

Since the size of the detector is taken into account in the reconstruction, the blurring that is caused by the non-ideal point like sensor can be avoided. This is demonstrated in Fig. 1, showing a comparison of simulated images of a phantom consisting of several uniformly heated spheres. One image used data from a cylindrically focused sensor with 5 mm width rotating at a distance of 20 mm around the center of the object. The image is reconstructed by using back projection over circles, the standard method for point like sensors. Due to the finite width of the sensor the outer sources are strongly blurred. By contrast, if an integrating detector with a ten times larger width of 50 mm is used for acquisition of signals from the same phantom, the resolution is similarly high for all the spheres in the phantom after the inverse Radon transform.

In this study, two detection setups are presented: A cylindrical, lens less detector employing a piezoelectric polymer film and an elliptical cylinder acting as acoustic reflector, combined with an optical interferometer as acoustic sensor.

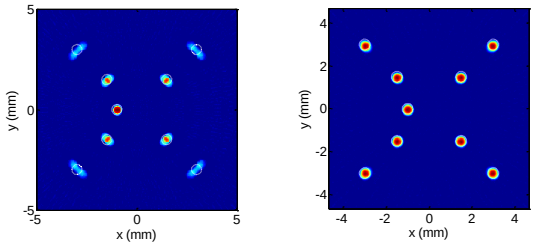

Fig. 1 Simulated photoacoustic images from signals measures with cylindrically focused detectors. Left: The detector has a width of 5 mm and a circular back projection is used. Right: The detector has a width of 50 mm and the inverse Radon transform is used for image reconstruction.

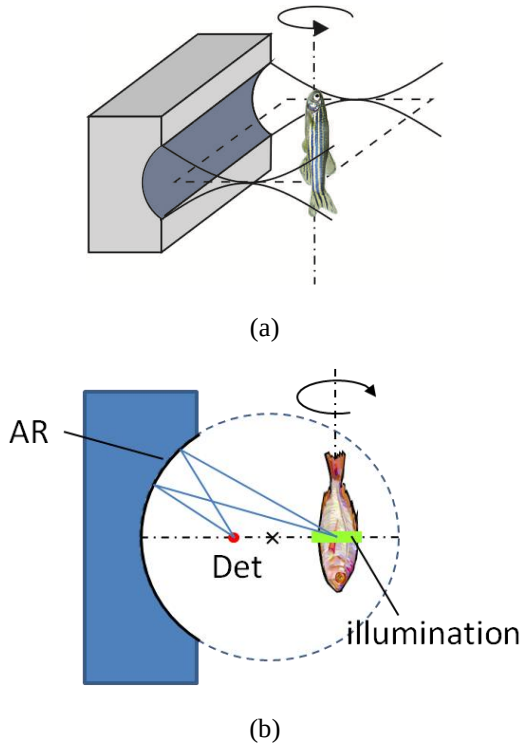

Fig. 2 Two implementations of integrating detectors for photoacoustic section imaging. (a) Integrating cylindrical detector made of a PVDF piezoelectric film. It has a width of 50 mm in direction of the cylinder axis and a height of 20 mm. The object is rotated relative to the cylinder during signal acquisition. (b) Optical detector employing a cylindrical acoustic reflector (AR). Acoustic signals are measured with an optical detector (Det).

Experimental setup

The two kinds of tomographic imaging devices are shown in Fig. 2. The lens less cylindrical detector in Fig.2(a) was a piezoelectric polymer film (PVDF) with 110 µm thickness on a concave cylindrical surface (Fig. 3). The length of the cylinder was 50 mm and its height 20 mm, giving a numerical aperture of NA = 0.5 considering the focal length of 20 mm. For data acquisition, the imaging object was rotated about an axis perpendicular to the cylinder axis. The imaging plane was irradiated from two sides in direction of the cylinder axis with pulses from an optical parametric oscillator (OPO), pumped by the frequency tripled output of a Q-switched Nd:YAG laser.

The second setup shown in Fig.2(b) consists of a cylindrical surface acting as an acoustic reflector. When properly aligned, acoustic waves emanating from one point in the photoacoustic source are collected at the acoustic detector, which is an optical beam within a Mach-Zehnder interferometer. The path of the acoustic waves for such an imaging configuration is indicated by the blue lines. In other words, the whole detection setup with the optical beam and the acoustic reflector focuses onto a line within the object. Due to the finite aperture of the reflector, the focusing volume is extended and it is possible to discriminate between different source positions via the time of flight of the acoustic signals. Again, the device integrates along one direction and the reconstruction uses the inverse Radon transform.

To demonstrate the performance of the imaging setup on a biological sample we took images of zebra fish. The fish were fixed in gelatin and were irradiated with a wavelength of 500 nm. For one scan, the fish were rotated in the focus of the lens by a total angle of 360°, with an increment of 0.9°. Before reconstruction using the inverse Radon transform, some signal processing was necessary to assure that the initially bipolar pressure signals always had a positive peak at the position of a photoacoustic source. For the experiments with the piezoelectric sensor the desirable signal shape was achieved after an Abel transform [3]. For the acoustic signals detected after reflection at the cylindrical mirror, a similar effect was achieved by applying a Hilbert transform.

Fig. 3 Photograph of the piezoelectric cylindrical sensor.

Results and discussion

Figure 4 shows images of a zebra fish, taken with the piezoelectric detector. The images taken with the optical detector are shown in Fig. 5. In both cases, a series of sections was imaged, showing various inner structures of the fish. In the experiment with the PVDF sensor also the black

stripes on the skin of the fish can be seen. For the optical detector experiment a mutation with no stripes was imaged, allowing a better discrimination of the inner structures. The imaging resolution, which was measured in separate experiments, was quite similar for both setups and amounted to about 100 µm in-plane and about 0.5 mm out of plane for the PVDF sensor and 1.2 mm for the optical sensor.

From the two demonstrated setups the one using optical detection has the slightly better sensitivity. Also, the signal fidelity is higher for the optical sensor, which takes advantage of the very flat frequency response of a fast photo detector. On the other hand, it requires accurate alignment of the optical detection beam relative to the acoustic reflector and the object to be imaged. Therefore, the handling of the piezoelectric sensor is easier.

In conclusion, two setups for achieving photoacoustic imaging of selected slices within an extended object are demonstrated. Due to the special reconstruction mechanism, which takes the extended length of the cylindrical elements into account, we can achieve accurate reconstructions with constant resolution over the imaging plane.

Acknowledgment

This work has been supported by the Austrian Science Fund (FWF), Project Nos. S10502-N20 and S10508-N20.

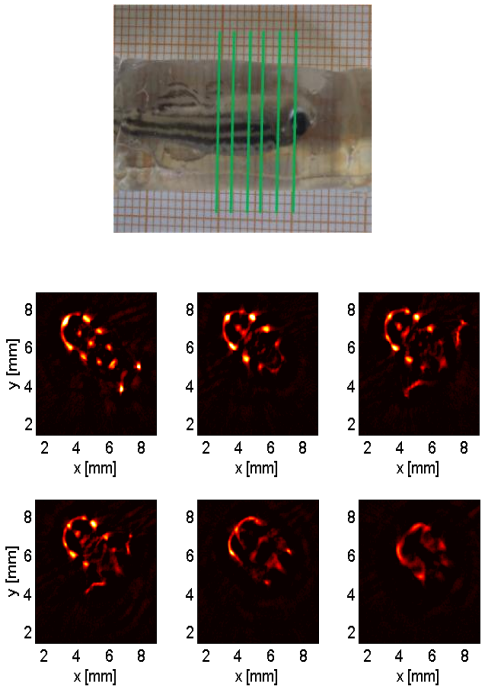

Fig.4 Photograph of the zebra fish imaged with the piezoelectric sensor and photoacoustic section images. The imaged sections are indicated by green lines.

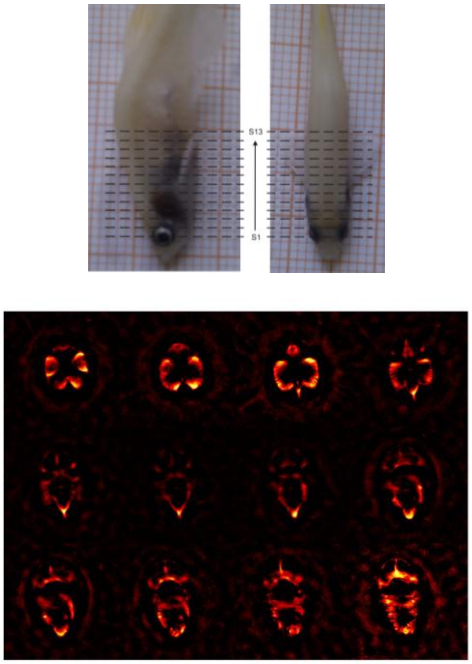

Fig.5 Photograph of the zebra fish imaged with the optical sensor and photoacoustic section images. The imaged sections are indicated by dashed black lines. In the photoacoustic images the sections are ordered row wise, starting from the head in the upper left corner.

References

1. M. H. Xu and L. V. Wang, "Photoacoustic Imaging in Biomedicine," Rev. Sci. Instrum. **77,** 041101 (2006).

2. R. Nuster, S. Gratt, K. Passler, G. Paltauf, and D. Meyer, "Photoacoustic section imaging using an elliptical acoustic mirror and optical detection," J. Biomed. Opt. **17,** 030503 (2011).

3. S. Gratt, K. Passler, R. Nuster, and G. Paltauf, "Photoacoustic section imaging with an integrating cylindrical detector," Biomed. Opt. Express **2,** 2973-2981 (2011).

4. M. H. Xu and L. V. Wang, "Analytic explanation of spatial resolution related to bandwidth and detector aperture size in thermoacoustic or photoacoustic reconstruction," Physical Review E **67,** 056605 (2003).

5. M. Haltmeier, O. Scherzer, P. Burgholzer, and G. Paltauf, "Thermoacoustic computed tomography with large planar receivers," Inverse Problems **20,** 1663-1673 (2004).

6. P. Burgholzer, C. Hofer, G. Paltauf, M. Haltmeier, and O. Scherzer, "Thermoacoustic tomography with integrating area and line detectors," IEEE Trans.Ultrason., Ferroelect., Freq.Contr. **52,** 1577-1583 (2005).